Cholesterol-Dependent Association of Caveolin-1 with the Transducin α Subunit in Bovine Photoreceptor Rod Outer Segments: Disruption by Cyclodextrin and Guanosine 5′-*O*-(3-Thiotriphosphate)†

Michael H. Elliott,*,‡ Steven J. Fliesler,§ and Abboud J. Ghalayini‡,||,⊥

Dean A. McGee Eye Institute, Department of Ophthalmology, Department of Cell Biology, and Oklahoma Center for Neuroscience, University of Oklahoma Health Sciences Center, Oklahoma City, Oklahoma 73104, and Saint Louis University Eye Institute and Department of Pharmacological and Physiological Science, Saint Louis University School of Medicine, St. Louis, Missouri 63104

Received November 12, 2002; Revised Manuscript Received April 18, 2003

ABSTRACT: Evidence suggests that caveolins, 21−24 kDa cholesterol-binding proteins that generally reside in specialized detergent-resistant membrane microdomains, act as signaling scaffolds. Detergent-resistant membranes isolated from rod outer segments (ROS) have been previously shown to contain the photoreceptor G-protein, transducin. In this report we show, by subcellular fractionation, that caveolin-1 is an authentic component of purified ROS. We demonstrate that caveolin-1 in ROS almost exclusively resides in low-buoyant-density, cholesterol-rich, detergent-resistant membranes that can be disrupted by cholesterol depletion using methyl-*β*-cyclodextrin (MCD). Cholesterol depletion was also observed to extract a pool of transducin α (Tα) from ROS membranes. Immunoprecipitation with anti-caveolin-1 revealed the association of Tα in the absence of T*βγ*. Treatment of ROS with MCD resulted in a 2-fold decrease in recovery of Tα in anti-caveolin-1 immunoprecipitates. This interaction was also completely disrupted when ROS were exposed to light in the presence of guanosine 5′-*O*-(3-thiotriphosphate) (GTP*γ*S), a nonhydrolyzable GTP analogue. In addition, caveolin-1/Tα association in the immune complex was disrupted by a peptide based on the primary sequence of the caveolin-1 scaffolding domain. Finally, we confirm the colocalization of caveolin-1 and Tα in photoreceptors by immunofluorescence microscopy. These results strongly suggest that the association between Tα and caveolin-1 occurs in cholesterol-rich, detergent-resistant membranes and is likely to be dependent upon the activation state of Tα.

The localization of signaling proteins to biological membranes is an important mechanism to regulate the specificity and fidelity of signal transduction pathways (*1*, *2*). Evidence suggests that cellular membranes are not uniform in the distribution of lipids but, instead, contain discrete, detergent-resistant, cholesterol- and sphingolipid-rich membrane microdomains floating in a sea of detergent-soluble phospholipids (*3*). The lipid environment of rafts tends to recruit fatty acyl-modified signaling proteins (*4*−*6*) and may act as organizing centers to localize a variety of signaling molecules (*2*). Detergent-resistant membranes (DRMs)[1] have been isolated from bovine photoreceptor rod outer segments (ROS) and have been shown to contain the photoreceptor G-protein, transducin, and cGMP-phosphodiesterase (c-GMP-PDE) (*7*) as well as the photoreceptor-specific regulator of G-protein signaling protein, RGS9-1 (*8*). In addition, DRMs containing the photoreceptor disk membrane protein ROM-1 have recently been purified from ROS disks (*9*). However, the mechanisms governing localization of proteins to raft domains in ROS are presently unknown.

Vertebrate phototransduction is a prototypical G-protein-coupled cascade in which light-mediated excitation of rhodopsin promotes the exchange of GDP for GTP on the transducin α subunit (Tα) and the dissociation of Tα/GTP from its *β*−*γ* subunit (T*βγ*), allowing activation of the effector enzyme, cGMP-PDE. This results in a decrease in cGMP concentration and subsequent closure of cGMP-gated cation channels leading to hyperpolarization of the photoreceptor membrane (*10*). A variety of complex mechanisms are likely to be involved in the regulation of phototransduction at the level of Tα (*11*). For example, acceleration of Tα GTPase activity by RGS9-1 leads to termination of Tα activation (*12*). In addition, the translocation of transducin from the site of photon capture, the outer segment, to the inner segment in response to light (*13*−*15*) affects amplification of the photoresponse (*16*). Another potentially important

† This work was supported by National Institutes of Health Grants EY11504, EY12190, EY07361, and F32 EY13674 and by unrestricted departmental grants from Research to Prevent Blindness, Inc.

* Corresponding author. Phone: 405-271-7351. Fax: 405-271-8128. E-mail: Michael-Elliott@ouhsc.edu.

‡ Dean A. McGee Eye Institute, Department of Ophthalmology, University of Oklahoma Health Sciences Center.

§ Saint Louis University Eye Institute and Department of Pharmacological and Physiological Science, Saint Louis University.

|| Department of Cell Biology, University of Oklahoma Health Sciences Center.

⊥ Oklahoma Center for Neuroscience, University of Oklahoma Health Sciences Center.

[1] Abbreviations: DRMs, detergent-resistant membranes; ROS, rod outer segments; c-GMP-PDE, cGMP-phosphodiesterase; GTP*γ*S, guanosine 5′-*O*-(3-thiotriphosphate); Tα, transducin α subunit; T*βγ*, transducin *β*−*γ* subunits; MCD, methyl-*β*-cyclodextrin.

10.1021/bi027162n CCC: $25.00
Published on Web 00/00/0000 PAGE EST: 11.9

mechanism of regulation may involve sequestration of Tα to specialized DRMs in photoreceptor membranes.

Tα is remarkably soluble relative to other G-protein α subunits (Gα) and can be extracted from ROS membranes without the use of detergents by washing with hypotonic, GTP-containing buffers (*17*, *18*). Although most Gα subunits are acylated at the amino terminus with myristic acid (C14:0), the amino termini of Tα subunits, among other photoreceptor proteins, are modified with a heterogeneous pool of saturated (C12:0 and C14:0) and unsaturated (C14:1 and C14:2) fatty acids (*19*−*21*). Heterogeneous acylation apparently influences the affinity of Tα for ROS membranes as demonstrated by differential extractability of heterogeneously acylated species by GTP-containing buffers (*22*). Results from our laboratory further demonstrate that a significant amount of Tα remains tightly associated with ROS membranes even after extensive washing with hypotonic buffers containing 100 μM GTP (*23*). Although currently unknown, it is possible that this tightly associated pool of Tα is localized to lipid raft membrane microdomains.

Caveolins, a family of 21−24 kDa cholesterol-binding membrane proteins enriched in specialized lipid rafts called caveolae, may enhance the association of acylated signaling molecules with DRMs and have been suggested to act as molecular scaffolds (*24*). G-protein α subunits associate with caveolins in a variety of cell types including photoreceptor-analogous olfactory cilia (*25*). Although caveolin-1 has recently been used as a marker for DRMs prepared from ROS membranes (*8*, *9*), there is controversy in the literature on whether caveolin-1 is an authentic component of ROS (*26*). In the current report, we demonstrate, unequivocally, by both biochemical and immunocytochemical methods, that caveolin-1 is a component of ROS membranes. Caveolin-1 was almost exclusively localized to cholesterol-rich, low-buoyant-density DRMs that also contained transducin subunits including Tα. Furthermore, Tα co-immunoprecipitated with caveolin-1, as our preliminary results suggested (*27*), in the absence of detectable Tβ. Both the cofractionation and co-immunoprecipitation of caveolin-1 and Tα are disrupted by the cholesterol-depleting agent methyl-β-cyclodextrin (MCD), suggesting that this association occurs in cholesterol-enriched DRMs. The interaction appears to depend on the activation state of Tα as light exposure of ROS in the presence of GTPγS inhibited recovery of Tα in caveolin-1 immunoprecipitates. In addition, using a peptide based on the primary sequence of the caveolin-1 scaffolding domain, we were able to elute Tα and caveolin-1 from anti-caveolin-1 and anti-Tα immunoprecipitates, respectively. To our knowledge, this is the first report demonstrating an in situ association between caveolin-1 and transducin in native ROS membranes.

EXPERIMENTAL PROCEDURES

Materials. Polyclonal antisera against caveolin-1 (N-20), caveolin-2 (H-96), Tα (K-20), Tβ (C-16), Gβ_{1-4} (T-20), Tγ (P-19), and rhodopsin kinase (C-20) were purchased from Santa Cruz Biotechnology, Inc. (Santa Cruz, CA). Polyclonal antibody against the C-terminus of Tα was from Calbiochem (San Diego, CA). Monoclonal antibody directed against Tα (clone 3) was from BD Transduction Laboratories (Lexington, KY). Monoclonal anti-opsin was a gift from Dr. Robert Molday (University of British Columbia). Monoclonal SV2 antibody was a gift from Dr. Erik Floor (University of Kansas). Polyclonal antibodies against the α1 and α1 subunits of the Na,K-ATPase were from Upstate, Inc. (Lake Placid, NY). A peptide based on the primary sequence of the scaffolding domain of caveolin-1 (amino acids 82−101, DGIWKASFTTFTVTKYWFYR) was synthesized by Research Genetics (Huntsville, AL). Glycine, Tween 20, sodium dodecyl sulfate (SDS), 2-mercaptoethanol, and prestained molecular weight markers were purchased from Bio-Rad. Gelcode Blue staining reagent was from Pierce (Rockford, IL). The silver-staining kit and Novex precast gels were from Invitrogen (Carlsbad, CA). [1,2,6,7-^{3}H]Cholesterol (60 Ci/mmol) was obtained from American Radiolabeled Chemicals, Inc. (St. Louis, MO). All other chemicals were purchased from Sigma.

Preparation of Bovine ROS. Bovine ROS were prepared from both dark- and light-adapted retinas on continuous sucrose gradients using a modification of the method of Zimmerman and Godchaux (*28*, *29*) as previously described (*30*). Briefly, 30 fresh bovine retinas (obtained from Mikkelson Beef, Inc., Oklahoma City, OK) were placed in 30 mL of ice-cold buffer A [10 mM Tris-HCl (pH 7.4), 100 mM NaCl, 2 mM $MgCl_2$, and 1 mM phenylmethanesulfonyl fluoride (PMSF)] containing 20% sucrose and stirred for 10−15 min using a plastic propeller fitted to a motor-driven homogenizer. The retinal suspension was centrifuged for 10 min at 800*g* at 4 °C in a Sorvall SS-34 rotor, and the supernatant obtained was saved. The pellet was resuspended in 25 mL of 20% sucrose in buffer A, the preceding was repeated two more times, and the pooled supernatants were centrifuged at 8000*g* at 4 °C for 30 min to obtain a crude ROS pellet. This pellet was resuspended in ∼10 mL of buffer A containing 60% sucrose and loaded at the bottom of six continuous gradients of 25−50% sucrose in buffer A. The tubes were centrifuged at 80000*g* for 85 min at 4 °C in a Beckman SW28 rotor and broken, and sealed ROS were collected from the gradients, pooled, diluted with an equal volume of buffer A containing 10% sucrose, and centrifuged at 27000*g* for 30 min at 4 °C. The final ROS pellets were resuspended in buffer A containing 10% sucrose (∼2.5 mg/mL) and frozen at −80 °C. For dark-adapted ROS, preparations were performed under dim red light.

To examine whether caveolin cofractionated with ROS proteins, the sealed and broken ROS collected from the initial gradient were pooled and layered at the bottom of a second continuous sucrose gradient and centrifuged at 80000*g* for an additional 85 min at 4 °C in a Beckman SW28 rotor. Following centrifugation, 1 mL fractions were collected from the bottom of the gradient and subjected to SDS−PAGE and immunoblot analysis.

Fractionation of Detergent-Resistant Low-Buoyant-Density Membranes (DRMs) from Bovine ROS Incubated with and without Methyl-β-cyclodextrin (MCD). DRMs were prepared according to the method of Seno et al. (*7*), with slight modification. Briefly, ROS (3 mg) were concentrated by centrifugation at 16000*g* for 20 min at 4 °C, resuspended in 10 mM Tris-HCl (pH 7.4), 100 mM NaCl, 5 mM $MgCl_2$, 1 mM EGTA, and 1 mM dithiothreitol (buffer B) with or without 15 mM MCD, and incubated for 1 h at 37 °C. Following incubation, ROS were solubilized with 1% Triton X-100 in buffer C and homogenized by three passes through

a 20-guage needle. The sucrose content was raised to 0.9 M by addition of 2.4 M sucrose in buffer C, and the solubilized homogenates were layered at the bottom of discontinuous sucrose gradients (0.8, 0.7, 0.6, and 0.5 M sucrose in buffer B). The gradients were centrifuged at 250000*g* for 20 h at 4 °C, and 0.5 mL fractions were collected from the top of the gradients.

Cholesterol and Lipid Phosphorus Analyses. Cholesterol analysis was performed by reverse-phase HPLC of the extracted, nonsaponifiable lipids, as described in detail previously (*31*). Prior to saponification, [^{3}H]cholesterol (0.1 μCi) was added to each sample to correct for differences in recovery efficiency and to serve as an internal chromatographic standard. Lipid phosphorus measurements were performed according to the method of Rouser et al. (*32*).

Washing of Bovine ROS with GTP and Incubation with MCD and GTPγS. Bovine ROS (200 μg) were diluted to a concentration of 1 mg/mL with ice-cold buffer A and centrifuged at 27000*g* for 20 min, and the resulting supernatant was collected (*isotonic* supernatant). The sedimented ROS membranes were then resuspended in the same buffer, divided into two equal volumes (100 μL each), and incubated in the presence or absence of 15 mM MCD for 1 h at 37 °C. Following incubation, the ROS were sedimented by centrifugation, and the resulting supernatants were subjected to SDS−PAGE and immunoblot analysis.

In other experiments, bovine ROS were washed in buffers of various ionic strengths as previously described (*23*) with slight modification. Bovine ROS (in buffer A containing 10% sucrose) were centrifuged at 27000*g* for 20 min at 4 °C, and the supernatant (isotonic wash) was collected. The ROS membrane pellet was sequentially washed two times in hypotonic buffer [10 mM Tris-HCl (pH 7.4), 3 mM $MgCl_2$, and 1 mM dithiothreitol], two times in hypotonic buffer containing 0.1 mM GTP, and three to five times in hypotonic buffer. For each wash, the ROS pellet was resuspended in the buffer and rotated for 15 min at 4 °C, followed by centrifugation at 27000*g* for 20 min. After washing, the ROS pellet was resuspended in hypotonic buffer, a 50 μL aliquot was removed for SDS−PAGE and immunoblot analysis, and the remaining washed ROS were split and incubated in the presence or absence of 15 mM MCD for 1 h at 37 °C. Following this incubation, the ROS membranes were centrifuged at 27000*g* for 20 min, the MCD and control supernatants were collected, and the ROS membrane pellets were resuspended in hypotonic buffer.

In additional experiments, 10 μM GTPγS (or an equal volume of water for controls) was added to dark-adapted ROS (in buffer A) under dim red light. ROS were immediately exposed to room light for 15 min at room temperature. Following light exposure, ROS were solubilized for immunoprecipitation as described below.

Immunoprecipitation. ROS (100−200 μg) were solubilized in 100−200 μL of solubilization buffer containing 10 mM Tris-HCl (pH 7.4), 50 mM NaCl, and 0.5 mM EDTA, with 1% Triton X-100 and 60 mM octyl glucoside, and centrifuged at 27000*g* for 30 min at 4 °C to remove particulate material. Supernatants were precleared by incubation with 50 μL of agarose-coupled protein A for 1 h at 4 °C with gentle rotation, followed by centrifugation at 2000*g* for 5 min. Precleared supernatants were incubated with 1−2 μg of polyclonal anti-caveolin or polyclonal anti-Tα for 2 h at 4 °C with gentle mixing, followed by the addition of 25 μL of agarose-coupled protein A and continued incubation for 1 h. The immune complexes were collected by centrifugation at 2000*g* for 5 min, washed four times with 0.4 mL of solubilization buffer, solubilized in 60 μL of SDS−PAGE sample buffer, and subjected to SDS−PAGE and immunoblot analysis.

In some experiments, immune complexes were washed as described with solubilization buffer and then incubated with 60 μL of caveolin-1 scaffolding domain peptide (100 μM) for 1 h at 4 °C with constant mixing. Following incubation, samples were centrifuged at 2000*g* for 5 min, and the supernatants were collected, diluted with 3× SDS−PAGE sample buffer, and subjected to SDS−PAGE and immunoblot analysis.

SDS−PAGE and Immunoblot Analyses. SDS−PAGE was performed according to the method of Laemmli (*33*), and separated proteins were transferred to Immobilon P membranes (0.45 μm) using MiniGenie or Genie electroblotters (Idea Scientific Co., Minneapolis, MN). Membranes were blocked for 1 h at room temperature or overnight at 4 °C with 5% bovine serum albumin in Tris-buffered saline (10 mM Tris-HCl, pH 7.4, 150 mM NaCl) containing 0.1% Tween 20 (TBST). Incubations with primary antisera were performed for 2 h at room temperature, followed by three washes with TBST. Blots were then incubated for 1 h with horseradish peroxidase-conjugated goat anti-rabbit or goat anti-mouse IgG and washed six times with TBST. Immunoreactions were detected using enhanced chemiluminescence substrates (ECL; Amersham Pharmacia Biotech, Piscataway, NJ). In some cases, blots were stripped by incubation, with gentle agitation, for 1 h at 50 °C in 100 mM Tris-HCl, pH 6.7, containing 100 mM 2-mercaptoethanol and 2% SDS. Blots were then washed four times with TBST, blocked, and reprobed as described.

Immunofluorescence Labeling of Bovine ROS Whole Mounts. Crude ROS with, in some cases, adherent inner segment blebs were prepared from freshly dissected bovine retinas by gentle homogenization through a Pasteur pipet in Hanks' balanced salt solution (Sigma Chemical Co., St. Louis, MO) buffered with 25 mM HEPES (pH 7.4) as described (*34*). Suspended cell fragments, allowed to adsorb for 3 min to Vectabond (Vector Laboratories, Burlingame, CA) treated glass slides, were fixed for 5 min with methanol at −20 °C. Prior to immunostaining, fixed cell fragments were dipped in chloroform, dried at room temperature, and washed three times with PBS. Slides were blocked for 1 h with PBS containing 0.3% BSA and 0.25% Triton X-100 and incubated overnight at 4 °C with a mixture of either polyclonal anti-Cav-1 (1:100) or polyclonal anti-Tα (1:1000) and monoclonal anti-opsin (1:200) or polyclonal anti-caveolin-1 and monoclonal anti-Tα (1:200), all diluted in PBS containing 0.3% BSA and 0.25% Triton X-100. As a control for Cav-1 antibody specificity, additional slides were incubated with polyclonal anti-Cav-1 that had been preadsorbed overnight at 4 °C with an excess of Cav-1 blocking peptide (Santa Cruz, sc-894P). Additional control slides were incubated in the absence of primary antisera. All slides were washed three times with PBS containing 0.25% Triton X-100, followed by incubation for 1 h at room temperature with a mixture of either Texas Red-coupled anti-mouse and FITC-coupled anti-rabbit or Texas Red-coupled anti-rabbit

and FITC-coupled anti-mouse secondary antibodies (Vector Laboratories, Burlingame, CA) diluted to 1:200 in the same buffer. After the slides were washed three times with PBS containing 0.25% Triton X-100, immunoreaction was examined on a Nikon Eclipse E800 microscope equipped with a digital camera. Images were captured, and color overlays were made using Metamorph image analysis software (Universal Imaging, West Chester, PA). When fluorescent labeling by primary antisera was compared to controls, all images were captured using identical microscope and camera settings so that the fluorescence intensities of the digital images quantitatively represent antibody binding.

Other Methods. Densitometric analysis of immunoblots was done using ONE-Dscan software (Scanalytics, Billerica, MA). Analyses of variance (ANOVA) and Student's *t*-tests were calculated using Microcal Origin with significance levels set at $P < 0.05$.

RESULTS

Cofractionation of Caveolin-1 with ROS Proteins. We first examined whether caveolin-1 was present in bovine ROS using an amino-terminal, peptide-specific polyclonal antibody. Broken ROS membranes and intact, sealed ROS prepared on a continuous sucrose gradient were pooled and fractionated a second time on a continuous sucrose gradient (*23*, *30*) in order to ensure that the presence of caveolin-1 was not due to contamination from other retinal cell membranes. As shown in Figure 1A, two peaks of total protein were observed which likely correspond to gradient fractions enriched in sealed ROS (fractions 17 and 18) or in broken ROS membranes (fractions 21 and 22). The major silver-stained band in all protein-containing fractions was the 36 kDa protein opsin (Figure 1B), confirmed by immunoreaction with monoclonal opsin antibody (Figure 1C). The characterization of gradient fractions as containing either sealed or broken ROS was further supported by the enrichment of the soluble protein, rhodopsin kinase (Grk-1), in fractions 17 and 18 (Figure 1D) and by the enrichment of the integral protein, opsin, in fractions 21 and 22 (Figure 1B). Tα, a peripheral membrane-associated protein, displayed a distribution similar to that of opsin with peak enrichment in the broken ROS membranes (Figure 1E). As apparent in Figure 1F, caveolin-1 immunoreactivity was also most abundant in fractions 21 and 22, consistent with it being associated with ROS membranes. To exclude the presence of potentially contaminating non-ROS membranes, gradient fractions containing both sealed and broken ROS (same fractions as in Figure 1) and a lysate containing 10 μg of bovine "whole retina and RPE" were subjected to immunoblot analysis with antibodies against α1- (Figure 2A) and α3-Na,K-ATPase isoforms (Figure 2B) and synaptic vesicle glycoprotein 2 (SV2; Figure 2C), markers of retinal pigment epithelium, photoreceptor inner segments, and synaptic vesicles, respectively. As shown in Figure 2, antibodies against ROS exclusion markers reacted robustly with the bovine "whole retina−RPE" but failed to react with any ROS gradient fractions. The presence of Tα was used as a positive marker for ROS (Figure 2D). Collectively, these data strongly indicate that caveolin-1 is an authentic component of photoreceptor ROS membranes and is not a non-ROS membrane contaminant.

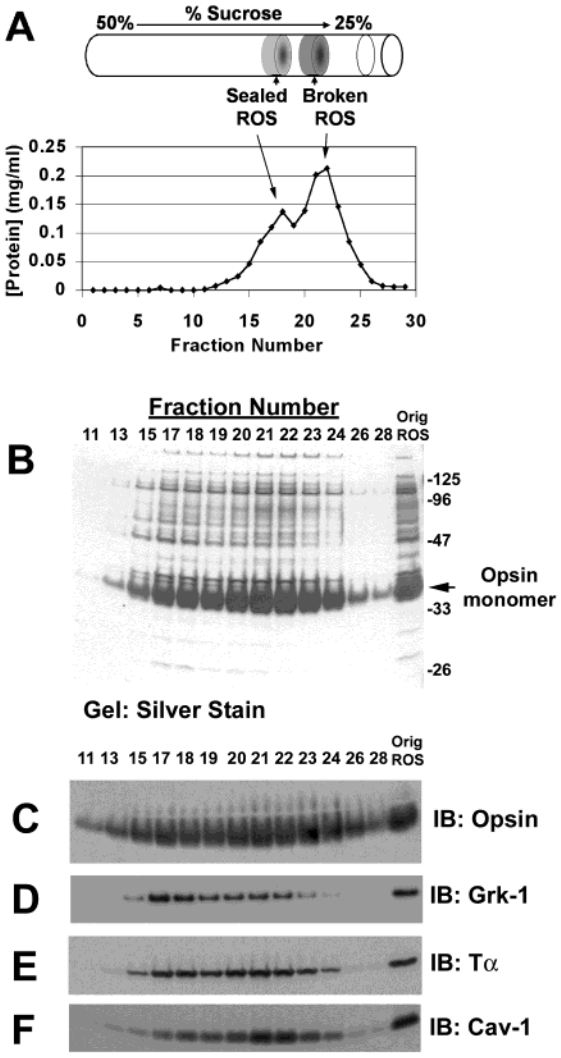

FIGURE 1: Caveolin-1 cofractionates with photoreceptor ROS membranes. ROS were prepared on two successive continuous sucrose gradients, and fractions were collected from the bottom of the second gradient as described under Experimental Procedures. (A) Total protein concentration as assessed by BCA protein assay. (B) Silver-stained gel of selected protein-containing fractions (15 μL each) subjected to SDS−PAGE. The lane designated Orig ROS was loaded with 10 μg of protein from ROS purified on the first continuous sucrose gradient. (C−F) Immunoblots of ROS gradient fractions (10 μL each) probed with polyclonal antibodies against opsin, rhodopsin kinase (Grk-1), Tα, and caveolin-1.

Caveolin-1 Cofractionates with a Pool of Transducin in Low-Buoyant-Density DRMs. Low-buoyant-density DRMs have recently been isolated from bovine ROS (*7*). DRMs enriched in caveolin are commonly purified by similar methods (*35*). In an attempt to determine whether DRMs isolated from ROS contained caveolin-1, light-adapted ROS were solubilized with Triton X-100 and subjected to discontinuous sucrose gradient centrifugation. Fractions were collected from the top of the gradients and subjected to SDS−PAGE and immunoblot analysis. A light-scattering band in the lower density portion of the gradient was visible (Figure 3A) and corresponded to fractions 2−4 as separated by SDS−PAGE and stained with Coomassie brilliant blue (Figure 3A). The protein composition of the low-buoyancy DRMs was similar to that recently described (*7*) and contained opsin (Figure 3A) and all three transducin subunits (Figure 3C) with a distinct peak of all proteins in fraction 3.

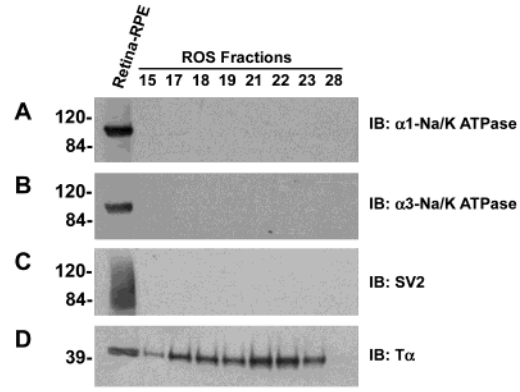

FIGURE 2: Purity of bovine ROS assessed by antibodies against non-ROS exclusion markers. ROS fractions (10 μg in peak fraction 22) and retina-RPE lysate (10 μg) were subjected to immunoblot analysis with the indicated antibodies.

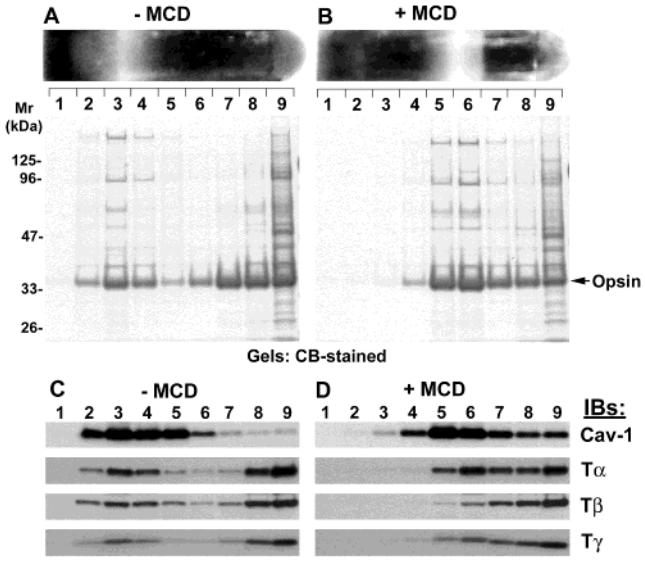

FIGURE 3: Effect of MCD on the localization of caveolin-1 and other ROS proteins in low-buoyant-density DRMs. ROS incubated in the absence (−MCD) or presence (+MCD) of 15 mM MCD were solubilized with 1% Triton X-100 and separated into low- and high-density fractions by discontinuous sucrose gradient centrifugation. Representative gradients were viewed by illumination prior to fractionation (A and B, upper panels). Fractions collected from the top of each gradient (top to bottom shown from left to right) were subjected to SDS−PAGE, and gels were stained with Coomassie blue (A and B, lower panels). (C, D) Immunoblots of corresponding fractions probed with antibodies against caveolin-1, Tα, Tβ, and Tγ.

Caveolin-1 immunoreactivity was almost exclusively localized to DRM fractions 2−5 with the most abundant immunoreactivity also in fraction 3 (Figure 3C). These results clearly demonstrate that caveolin-1 associates almost entirely with low-buoyant-density DRMs and cofractionates with a specific pool of Tα.

In parallel experiments, DRMs were prepared (simultaneously with those shown in Figure 3A) from ROS previously incubated with the cholesterol-sequestering agent, MCD, a treatment that disrupts caveolar membranes (*36*−*38*). As shown in Figure 3B, MCD treatment for 1 h resulted in a dramatic loss of the low-buoyant-density, light-scattering band (Figure 3B) accompanied by a shift in the distribution of proteins to higher density sucrose fractions (Figure 3B,D). The concomitant shift in both caveolin-1 and transducin to

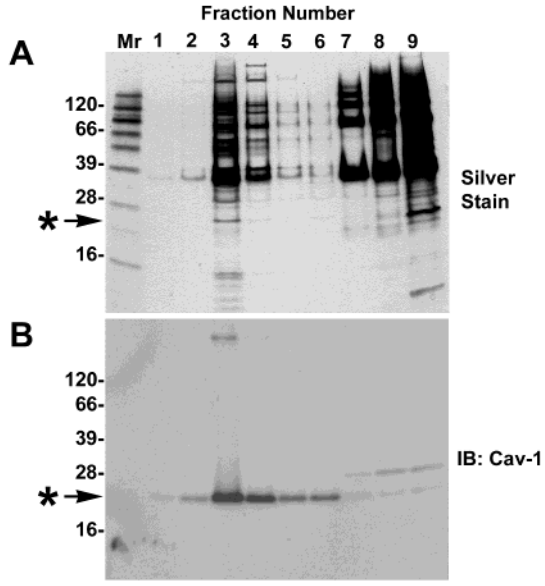

FIGURE 4: Silver staining and immunoblot analysis of DRM gradient fractions. Equal volumes (20 μL) of each DRM gradient fraction were subjected to reducing SDS−PAGE (without boiling) and either silver staining (A) or immunoblot analysis with a polyclonal caveolin-1 antibody (B). The asterisk denotes a DRM-enriched protein band at the relative molecular weight of caveolin-1 detectable on the silver stained gel (A) and immunopositive caveolin-1 on the parallel immunoblot (B).

higher density fractions (Figure 3C,D) following MCD treatment shows that their colocalization to DRMs is disrupted presumably by the cholesterol-depleting actions of MCD.

On silver-stained gels, a protein band with the relative molecular weight of caveolin-1 (M_r ≈24000, indicated by an asterisk) was detectable in DRMs (Figure 4A) but was not detectable by Coomassie staining (not shown). This band appeared to be enriched in the peak DRM fraction (fraction 3) and was also faintly detectable in fraction 4. The appearance of this band corresponded well with caveolin-1 immunoreactivity on a parallel immunoblot (Figure 4B), which was not detected in non-DRM fractions (Figure 4B, fractions 6−8). However, we cannot rule out the presence of another protein(s) that is comigrating with caveolin-1 on silver-stained gels of DRM fractions.

To estimate the relative distributions of transducin and caveolin-1 in DRM fractions, we performed densitometric analyses of immunoblots from three independent DRM preparations. The percent totals of Tα, Tβ, and Tγ in each fraction are superimposed on the percent total of caveolin-1 (Figure 5). As shown, DRM fractions (fraction 2−4) contained ~34% of the total Tα (black columns), which is in good agreement with the results of Seno et al. (*7*). The bulk of the remaining Tα (60% of the remaining 66%) was present in "non-DRM" fractions 6−9. Importantly, fractions 2−4 also contained more than 75% of the total caveolin-1. The pattern of partitioning of Tβ and Tγ subunits to DRMs is similar to that of Tα. When the relative amounts of each transducin subunit in the peak caveolin-containing fractions (fractions 2−4) were compared quantitatively, there was 10% more Tα than Tβ and 14% more Tα than Tγ.

Low-Buoyant-Density DRMs Isolated from ROS Are Enriched in Cholesterol. The localization of caveolin-1 to low-buoyant-density DRMs and the disruption of this

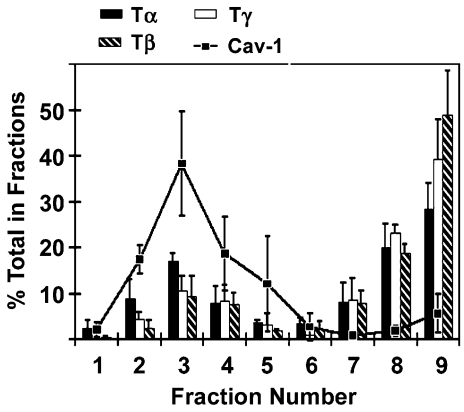

FIGURE 5: Densitometric analysis of the distribution of transducin subunits and caveolin-1 in DRM gradient fractions. Immunoblots of gradient fractions from three independent DRM preparations were subjected to densitometric analysis to quantify the fractionation of transducin subunits and caveolin-1 in each fraction as a function of the total in all fractions. Bars represent the percent total (mean ± SD, $n = 3$) for Tα (black columns), Tβ (white columns), and Tγ (crosshatched columns) superimposed on the percent total of caveolin-1 (black squares) in each fraction.

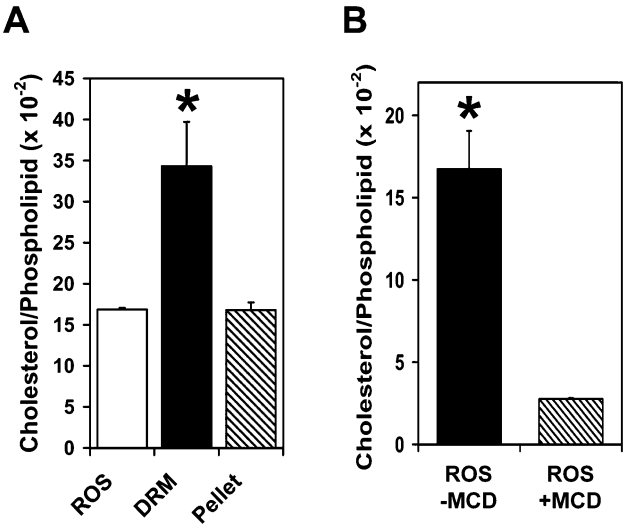

FIGURE 6: Cholesterol content of DRMs and ROS incubated with MCD. Cholesterol and lipid phosphorus determinations were made as described in Experimental Procedures. (A) Cholesterol:phospholipid molar ratios (mean ± SD) were calculated for ROS, DRM (fraction 3), and pellet (fraction 9). *, significantly different; $P < 0.001$, one-way ANOVA, $n = 3$. (B) Cholesterol:phospholipid molar ratios (mean ± SD) were calculated for control (−MCD) and MCD-incubated (+MCD) ROS. *, significantly different; $P < 0.05$, paired *t*-test, $n = 3$.

localization by MCD suggested that DRMs prepared from ROS are enriched in cholesterol. In an effort to confirm this hypothesis, we compared the cholesterol:phospholipid ratio in fraction 3 (DRMs) to fraction 9 (pellet) and to the original ROS starting material (Figure 6A). The cholesterol:phospholipid molar ratio of ROS membranes was found to be 0.16, in agreement with recently reported values for bovine rod disk membranes (*39*). Importantly, there was a significant ($P < 0.001$, one-way ANOVA, $n = 3$), 2-fold increase in the cholesterol:phospholipid ratio of the DRM fraction relative to both the pellet fraction and the original ROS, in good agreement with the increase in cholesterol:phospholipid ratio recently reported for DRMs isolated from ROS disk membranes (*9*). However, our cholesterol:phospholipid ratios are higher than those reported by Boesze-Battaglia et al., perhaps due to differences in the methods employed to measure both cholesterol and phospholipids. The cholesterol content of the pellet fraction was almost identical to the original ROS starting material. These data demonstrate unequivocally that DRMs isolated from bovine ROS are enriched in cholesterol.

The effect of MCD incubation on the cholesterol content of ROS is demonstrated in Figure 6B. Incubating ROS with 15 mM MCD for 1 h at 37 °C resulted in a significant ($P < 0.01$, paired *t*-test, $n = 3$), 84% decrease in cholesterol content. The efficiency of cholesterol depletion by MCD was similar to that recently reported for isolated rod disks (*9*, *39*). In MCD-treated ROS, we observed a small (∼3%) but insignificant ($P = 0.13$, paired *t*-test, $n = 3$) decrease in phospholipid content, comparable to what has been previously reported (*39*). Indeed, the profound reduction in the cholesterol:phospholipid ratio upon treatment with MCD, observed both in this study and in that reported by Niu et al. (*39*), must be due specifically to the loss of cholesterol, as any significant loss of phospholipid would have *increased* the ratio. These results confirm that the cholesterol content of ROS membranes is dramatically reduced by incubation with MCD at concentrations previously shown to disrupt the fractionation of DRMs (see Figure 3). Therefore, the increased cholesterol content of DRMs may influence the partitioning of protein components to membrane microdomains in ROS.

MCD Extracts Tα from ROS Membranes and Disrupts Caveolin-1/Tα Complexes. Incubation of membranes with MCD has been shown to enhance the Triton solubility of previously insoluble proteins (*40*, *41*) and, in some instances, to directly solubilize membrane-associated proteins in the absence of detergents (*42*). As incubation of ROS with MCD dramatically reduced the buoyancy of DRM-associated proteins (see Figure 3B,D), we examined the effect of MCD treatment on the extractability of transducin from ROS membranes. For these experiments, ROS (Figure 7A, Orig ROS) in isotonic buffer A with 10% sucrose (see Experimental Procedures) were centrifuged, yielding ROS membranes and isotonic supernatants (Figure 7A, Iso Sup). The ROS membranes were then incubated in the presence or absence of MCD in isotonic buffer at 37 °C for 1 h. Following incubation, the ROS membranes were centrifuged and the resulting supernatants subjected to SDS−PAGE and immunoblot analysis (Figure 7A, + or −MCD Sup). As shown, MCD incubation led to increased recovery of Tα in supernatant fractions without extraction of caveolin-1 (Figure 7A).

In other experiments, ROS membranes were washed extensively with hypotonic and hypotonic/GTP-containing buffers prior to incubation of membranes with or without MCD. Under a similar washing paradigm (without MCD incubation), we had previously observed the retention of a significant pool of Tα on ROS membranes (*23*). As expected, abundant recovery of Tα was observed following washes with 0.1 mM GTP (Figure 7B, lanes 5 and 6). However, following incubation of washed ROS membranes with MCD, significantly more Tα was released into the supernatant fraction than was released in control incubations (Figure 5B, lanes 10 and 11). These results indicate that a specific pool of Tα that is tightly associated with ROS membranes can

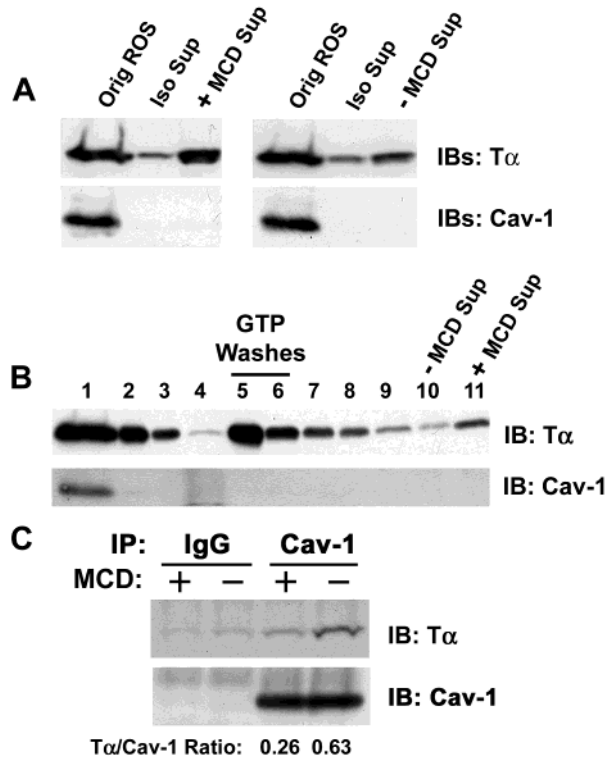

FIGURE 7: Extraction of Tα from ROS membranes and disruption of caveolin-1/Tα complexes by MCD. (A) ROS starting material (1 mg/mL; Orig ROS) was split into equal parts and centrifuged, and initial isotonic supernatants (250 μL; Iso Sup) were collected. ROS membrane pellets were then incubated at 37 °C for 1 h in 250 μL of isotonic buffer supplemented with or without MCD and centrifuged to collect the supernatant fractions (+MCD Sup and −MCD Sup). ROS (8 μg) and equal volumes (20 μL) of supernatant fractions were subjected to SDS−PAGE and immunoblot analysis using polyclonal anti-Tα and anti-caveolin-1 antisera. (B) ROS (lane 1) were washed sequentially with hypotonic buffers (lanes 2−4), hypotonic buffers containing 0.1 M GTP (lanes 5 and 6), and hypotonic buffers (lanes 7−9). Washed ROS membranes (200 μg/incubation) were then incubated in the absence (lane 10) or presence (lane 11) of MCD, and supernatant fractions were collected following centrifugation. Equal volumes (15 μL) of wash fractions were resolved on 10% SDS−PAGE gels and subjected to immunoblot analysis using polyclonal antibodies against Tα and caveolin-1. (C) ROS incubated in the presence or absence of MCD were immunoprecipitated with polyclonal anti-caveolin-1 or normal rabbit IgG as described in Experimental Procedures. Immune complexes were solubilized in SDS−PAGE sample buffer, resolved on 10% gels, and subjected to immunoblot analysis with monoclonal anti-Tα and polyclonal anti-caveolin-1. The ratio of Tα/caveolin-1 in the immune complexes shown was determined by densitometric analysis.

be extracted by cholesterol depletion but not by GTP. Although stringent GTP extraction and MCD incubation both resulted in substantial release of Tα from ROS membranes, a pool of Tα still remained associated with ROS pellets (not shown), suggesting the involvement of other unknown mechanisms of interaction between Tα and ROS membranes.

Although generally thought of as an integral membrane protein (*43*), caveolin-1 has recently been localized to a soluble lipid complex in cytosolic fractions of some cell types (*44*). However, in ROS, under all washing paradigms studied, caveolin-1 remained associated with pelleted membranes following centrifugation (Figure 7A,B).

On the basis of the observed MCD-sensitive cofractionation of Tα and caveolin-1 to DRMs and because of several reports of caveolin/G-protein interactions (*25*, *45*, *46*), we hypothesized that caveolin-1 and Tα might be associated as an immunoprecipitable complex in ROS and that this complex might be sensitive to cholesterol content. Although DRMs are insoluble in Triton X-100, they can be effectively solubilized with octyl glucoside (*47*−*49*). Therefore, all immunoprecipitations were carried out with ROS solubilized with a combination of Triton X-100 and octyl glucoside. Using an amino-terminal-specific polyclonal antibody, caveolin-1 was immunoprecipitated from ROS that had been incubated in the presence or absence of MCD. As shown in Figure 7C, Tα was recovered in caveolin immunoprecipitates. However, MCD treatment resulted in a greater than 2-fold reduction in Tα recovery, suggesting that cholesterol depletion disrupts the caveolin/Tα interaction.

Association of Tα but Not Tβ with Caveolin-1 in ROS. On the basis of our observation that Tα could be recovered in caveolin-1 immunoprecipitates and that a pool of Tβ also cofractionated in DRMs, we examined whether Tβ might also be present in the immune complex containing caveolin-1 and Tα. Panels A and B of Figure 8 show representative caveolin-1 immunoprecipitations. In addition, duplicate caveolin-1 immunoprecipitations along with the corresponding ROS starting materials are shown in Figure 8B. As demonstrated by these experiments and in agreement with our earlier data (see Figure 7C), Tα was recovered by immunoprecipitation with anti-caveolin-1. However, although robust immunoreaction to Tβ was observable in the ROS starting material (Figure 8B, middle panel), neither Tβ (Figure 8A and 8B) nor Tγ (not shown) was detected in anti-caveolin-1 immunoprecipitates, suggesting that caveolin-1 associates with Tα when it is dissociated from Tβγ. Tα was not detected in control immunoprecipitates using nonimmune IgG instead of anti-caveolin-1, showing the specificity of the co-immunoprecipitation. These data collectively suggest that the association of Tα with caveolin-1 may competitively preclude its association with Tβγ.

In other experiments, ROS were immunoprecipitated with anti-caveolin-1 and anti-Tα, and the immune complexes were subsequently incubated with a synthetic peptide based on the primary sequence of the caveolin-1 scaffolding domain. The peptide eluates were collected and subjected to SDS−PAGE and immunoblot analysis. If caveolin-1 and Tα associate through the scaffolding domain, then this peptide might disrupt this interaction, resulting in the affinity elution of the associated protein from the immune complexes. As demonstrated in Figure 8C, the scaffolding domain peptide was able to elute bound caveolin-1 and Tα from anti-Tα immunoprecipitates and anti-caveolin-1 immunoprecipitates, respectively. It is important to point out that no caveolin-1 was eluted from the anti-caveolin-1 immune complex and no Tα was eluted from the anti-Tα complex (Figure 8C). These results suggest that the recovery of either protein from the immune complex is the result of disrupting the interaction between Tα and caveolin-1 and not from elution of the entire immune complex. This strongly suggests that the scaffolding domain is involved in the interaction of caveolin-1 and Tα. It is noteworthy that the putative caveolin binding motif (*50*) falls between the switch I and switch II domains in Tα (Figure 6D) and overlaps two important Tα/Tβγ contact sites (*51*). Therefore, the associations between caveolin and Tα and between Tβγ and Tα might be mutually exclusive,

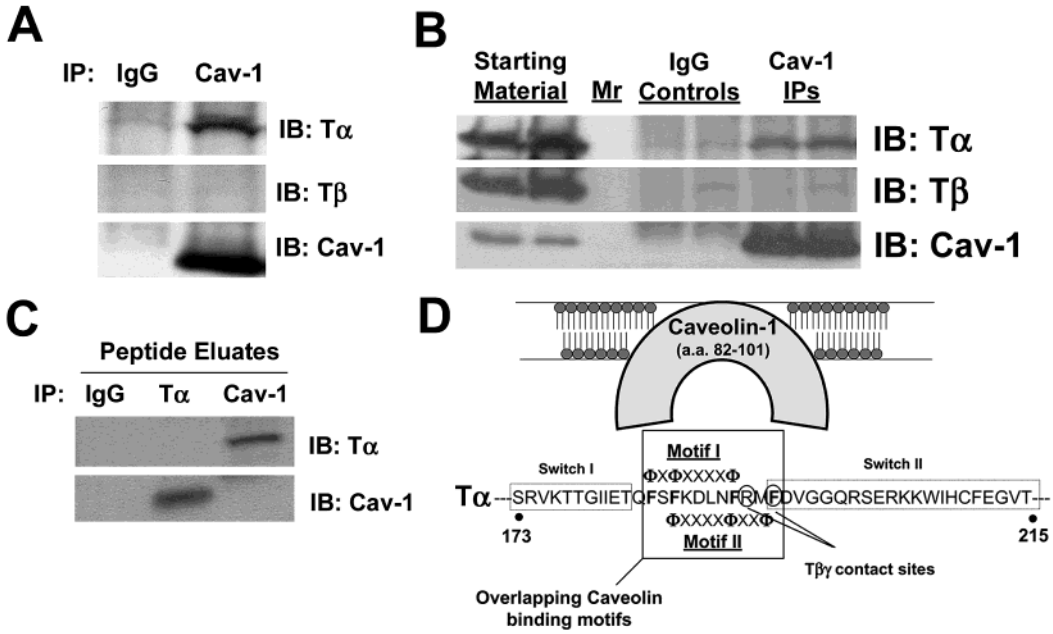

FIGURE 8: Tα associates with caveolin-1 in the absence of T*β*. (A) ROS were solubilized with 1% Triton X-100 in combination with 60 mM octyl glucoside and immunoprecipitated with polyclonal anti-caveolin-1 or normal rabbit IgG as described in Experimental Procedures. Immune complexes were subjected to SDS−PAGE and immunoblot analysis using antibodies against Tα, T*β*, and caveolin-1. (B) Additional caveolin-1 immunoprecipitations (shown in duplicate) with 10 μg of the corresponding solubilized ROS starting material for comparison. M_r = molecular weight standards. (C) Immunoblots of caveolin-1 and Tα immunoprecipitates eluted with 100 μM caveolin-1 scaffolding domain peptide as described in Experimental Procedures. The soluble eluates were subjected to SDS−PAGE, and immunoblots were probed with antibodies against Tα and caveolin-1. (D) Diagram of caveolin binding motifs within the sequence of Tα that is suggested to interact with the caveolin scaffolding domain. Note the presence of two T$\beta\gamma$ contact sites adjacent to motif I and within motif II.

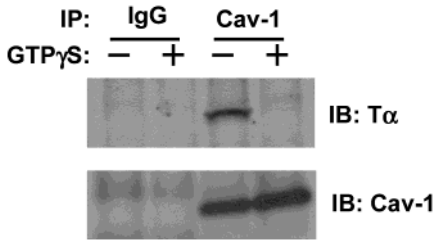

FIGURE 9: Effect of GTPγS on the interaction between caveolin-1 and Tα. Dark-adapted ROS were exposed to room light in the absence (−) or presence (+) of 10 μM GTPγS, solubilized, and immunoprecipitated with anti-caveolin-1. The upper panel shows an immunoblot of the immune complexes with anti-Tα (monoclonal). The lower panel shows the same immunoblot reprobed with anti-caveolin-1 (polyclonal). These blots are representative of two independent experiments.

consistent with the observed recovery of Tα in caveolin-1 immunoprecipitates in the absence of T$\beta\gamma$.

Effect of GTPγS on Caveolin/Tα Association. Reports from two independent laboratories demonstrated that the fractionation of Tα to DRMs in a light-dependent manner was inhibited by the nonhydrolyzable GTP analogue, GTPγS (*7*, *8*). Since caveolin-1 is almost exclusively localized to DRMs, we hypothesized that its interaction with Tα might be influenced by GTPγS. To test this hypothesis, dark-adapted ROS were exposed to light for 15 min in the presence or absence of 10 μM GTPγS, solubilized, and immunoprecipitated with anti-caveolin-1, and recovery of Tα in the immune complex was determined by immunoblot analysis. As shown in Figure 9, incubation with GTPγS resulted in almost complete loss of recovery of Tα in the immune complex, indicating the disruption of interaction between caveolin-1 and Tα by GTPγS. These results suggest that the activation of Tα hinders its ability to associate with caveolin-1.

Immunolocalization of Caveolin-1 in Isolated Photoreceptors. In an attempt to determine the localization of caveolin-1 in photoreceptors, we used immunofluorescence microscopy of isolated, whole-mounted bovine photoreceptors (*34*). Photoreceptors prepared in this manner typically contain morphologically distinct outer segments (labeled ROS in Figure 10A) with inner segment blebs (RIS, Figure 10A) adhering to the connecting cilium observable by phase-contrast microscopy (Figure 10A,D,G). Photoreceptor identity was confirmed by dual labeling whole mounts with monoclonal anti-opsin followed by Texas Red-coupled anti-mouse IgG (Figure 10B,E,H). Caveolin-1 immunoreactivity was observable throughout inner segment blebs and in ROS where labeling was distinctly punctate (Figure 10C). The specificity of caveolin-1 immunolabeling was confirmed by adsorbing the caveolin-1 antibody to its peptide antigen prior to immunostaining photoreceptor whole mounts. As demonstrated, peptide blocking dramatically reduced detectable caveolin-1 (Figure 10F) without interfering with opsin immunoreactivity (Figure 10E). The localization of caveolin-1 in bovine photoreceptors was remarkably similar to that observed for Tα (Figure 10I). The colocalization of caveolin-1 and Tα was confirmed by dual labeling of dissociated bovine photoreceptors with polyclonal anti-caveolin-1 (Figure 10J) and monoclonal anti-Tα (Figure 10K). An image showing the overlaid caveolin-1 and Tα immunoreactivity is presented in Figure 10L. As these photoreceptors were isolated from light-adapted retinas, the detection of significant Tα immunoreactivity in inner segment blebs is consistent with the light-dependent translocation of this protein from ROS to RIS (*13*−*16*).

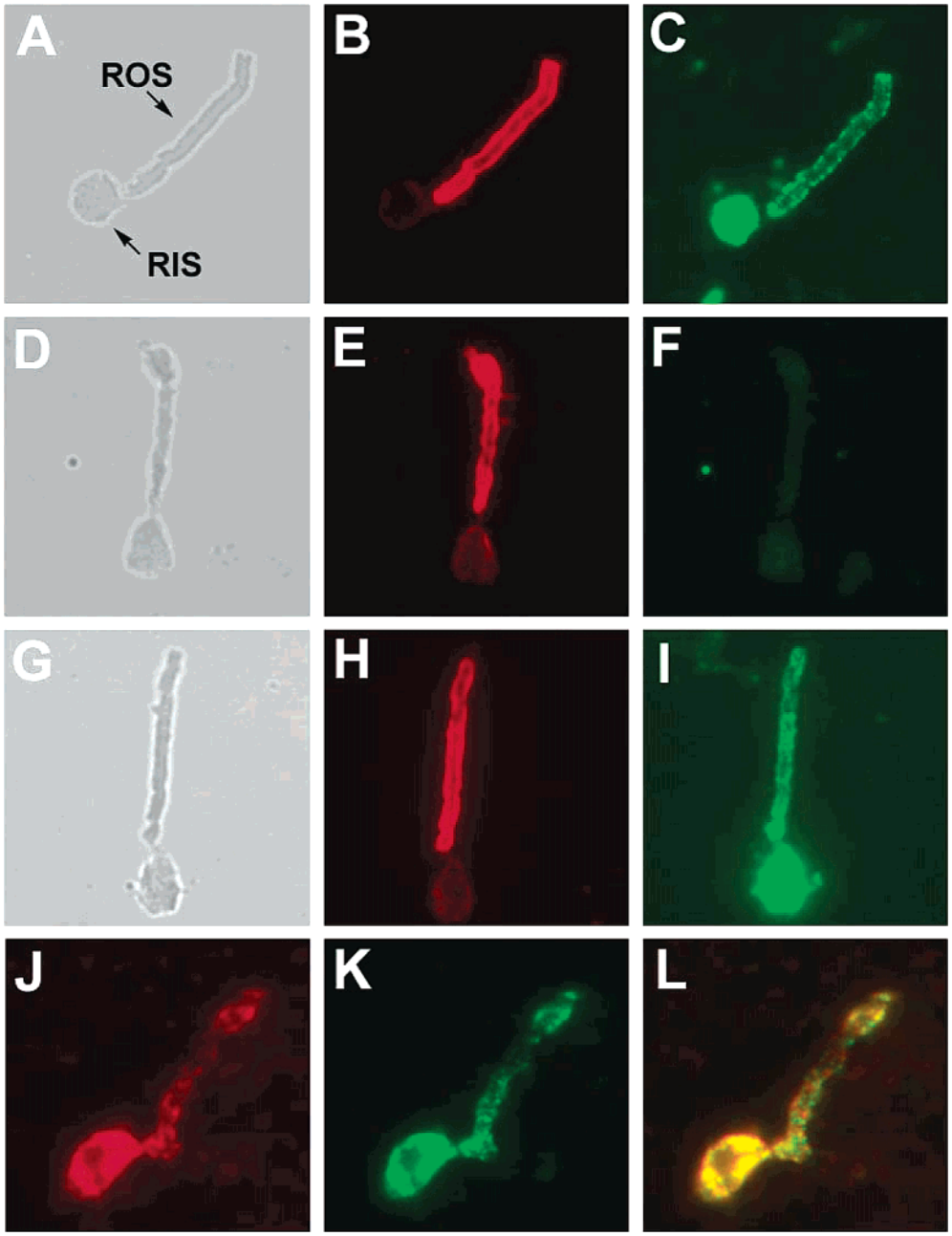

FIGURE 10: Immunolocalization of caveolin-1 and Tα in isolated bovine photoreceptors. Dissociated bovine photoreceptors were prepared for immunofluorescence microscopy as described in Experimental Procedures. Phase-contrast images of photoreceptors (A, D, G) dual-labeled with monoclonal anti-opsin (B, E, H) and either polyclonal anti-caveolin-1 (C, J), polyclonal anti-caveolin-1 preadsorbed against its peptide epitope (F), or polyclonal anti-Tα (I, K). Image overlay of a dissociated bovine photoreceptor dual-labeled with polyclonal anti-caveolin-1 and monoclonal anti-Ta (L).

DISCUSSION

A substantial body of evidence suggests that distinct pools of signaling proteins partition to cholesterol- and sphingolipid-enriched DRMs (*1*−*3*) and to specialized DRMs containing caveolin (*52*, *53*). In photoreceptor biology, the localization of phototransduction proteins to lipid raft microdomains has received attention only recently (*7*−*9*, *27*). In the current paper, we expand upon these results by demonstrating that DRM fractions isolated from bovine ROS are enriched in cholesterol and contain the scaffolding protein, caveolin-1, and that a specific pool of Tα interacts with caveolin-1 in bleached ROS preparations in a cholesterol- and GTPγS-dependent manner. Although caveolin-1 and rhodopsin kinase have been shown to interact in vitro (*54*), our report is the first to demonstrate the specific association of caveolin-1 with a photoreceptor-specific protein (Tα) in native ROS membranes. These results suggest that caveolin-1 may play an important role in localizing Tα to DRMs and, therefore, may play a significant role (the details of which are yet to be elucidated) in regulation of the phototransduction signaling cascade.

The caveolin-1 detected in ROS preparations behaves similarly to caveolin-1 in other cell types (*53*); namely, (1) it is tightly associated with membranes, (2) it is dramatically localized to cholesterol-enriched, Triton-insoluble, low-buoyant-density DRMs, and (3) it can associate with a Gα subunit. Caveolin-1 immunoreactivity has been localized to retinal pigment epithelial cells (*55*) and to photoreceptor

synaptic ribbons but was not detected in ROS preparations by immunoblot analysis (*26*). In contrast, we find robust caveolin-1 immunoreactivity cofractionating with opsin in bovine ROS fractions. The purity of ROS preparations used was verified by the absence of several markers of non-ROS proteins (α1 and α3 isoforms of the Na,K-ATPase and SV2). Differences in immunoblot detection sensitivities might explain the discrepancy between our results and the previously published report by Kachi et al. (*26*). We used a luminol-based chemiluminescence detection system (ECL; Amersham-Pharmacia Biotech.) which is reportedly 10-fold more sensitive than the dye-conjugated system (*56*) used in this earlier study (*26*). In addition to biochemical fractionation, we were able to colocalize caveolin-1 and Tα to ROS and to photoreceptor inner segment blebs using immunofluorescence microscopy. Moreover, Nair et al. (*8*) and Boesze-Battaglia et al. (*9*) recently used caveolin-1 immunoreactivity as a marker for DRMs isolated from bovine ROS and ROS disk membranes, respectively. Kachi et al. (*26*) had reported that caveolin-1 was undetectable in ROS, and neither Nair et al. (*8*) nor Boesze-Battaglia et al. (*9*) presented immunocytochemical evidence for the presence of caveolin-1 in ROS or biochemical evidence addressing the purity of the preparations used in their studies. Given that our report is the first to demonstrate a protein−protein interaction between caveolin-1 and Tα, it was imperative in our studies to unequivocally demonstrate that caveolin-1 is a bona fide ROS component using both biochemical and immunocytochemical approaches. Our findings are in agreement with the report of Nair et al. (*8*) on the presence of caveolin-1 in ROS (and ROS DRMs). However, the resolution limits of immunofluorescence microscopy do not allow us to confirm the localization of caveolin-1 to ROS disk membranes as reported by Boesze-Battaglia et al. (*9*).

Our results on the localization of Tα to DRMs are also consistent with those previously reported (*7*−*8*). We expand upon these findings by demonstrating that the association of Tα with low-buoyant-density DRMs is influenced by cholesterol content. In addition, our report is the first to demonstrate an interaction between Tα and caveolin-1 in native ROS membranes. Like many heterotrimeric Gα subunits, Tα contains caveolin binding motifs suggested to interact directly with the caveolin scaffolding domain (*50*). In Tα (see Figure 8D), this binding motif (^{185}FSFKDLNFRMF^{195}) overlaps at least two residues important for interaction with Tβγ (*51*). If caveolin-1 and Tα interact directly via the scaffolding domain of caveolin-1 and the caveolin binding motif of Tα, as is strongly suggested by our peptide elution data, then this interaction might competitively block or disrupt the association of Tα with Tβγ, consistent with the recovery of Tα, but not Tβγ, in caveolin-1 immunoprecipitates (see Figure 8A,B). In support of this hypothesis, $G\alpha_q$ has also been shown to co-immunoprecipitate with caveolin-1 in the absence of its βγ subunit (*57*). Furthermore, the association of caveolin-1 and expressed Gα in MDCK cells does not require coexpression of Gβγ (*45*). The absence of Tβ from anti-caveolin immunoprecipitates suggests that it is either not associated with Tα in DRMs or that it is associated with a pool of Tα not in complex with caveolin-1. Our data, however, do not rule out the presence of additional protein components in caveolin/Tα immune complexes.

Although Tβγ is not associated with caveolin-1, it is detectable in DRM fractions (see Figures 3 and 4) as previously observed by Seno et al. (*7*). This finding is surprising because the prenyl group on the Gγ subunit of G_i has been shown to inhibit its partitioning (and that of heterotrimeric G_i) to DRMs in model membrane systems (*5*). On the basis of our densitometric analyses, there is more Tα (34% of total) partitioning to DRMs than Tβ (24% of total) and Tγ (20% of total) (Figure 4). However, as discussed above, it appears that any Tα that is associated with caveolin-1 is not likely to be associated with Tβγ. This suggests that the Tβγ that partitions into DRMs is either associated with DRM-localized Tα that is not interacting with caveolin-1 or that Tβγ is interacting with some other DRM-associated protein. Alternatively, it is possible that the unique lipid composition of DRMs derived from ROS might allow partitioning of Tβγ dimers to these membrane microdomains.

Although other G-protein α subunits have been shown to interact with caveolin-1 (*45*, *57*), to our knowledge, this is the first study to show the endogenous interaction of a Gα subunit that is not palmitoylated. Dual acylation, e.g., N-terminal myristoylation coupled with thiopalmitoylation, has been shown to be necessary for the association of $G_{i1}\alpha$ with DRMs (*5*) and $G_o\alpha$ with caveolin-enriched membranes (*59*). Furthermore, dual acylation of a 32 amino acid N-terminal peptide derived from $G_{i1}\alpha$ is required for co-immunoprecipitation with caveolin (*60*). These findings have led to the conclusion that palmitoylation is necessary for caveolin-1/Gα interactions. However, Tα, unlike most Gα subunits, does not contain a palmitoylation site (*61*). Our results clearly demonstrate that Tα is localized to cholesterol-rich DRMs and is present in a complex with caveolin-1 in ROS preparations, suggesting that, at least for Tα, dual acylation is not required for association with caveolin-1. It is important to note that specific lipid modifications of Gα subunits are not required for interaction with the caveolin scaffolding domain, in vitro (*45*).

In this report, we have also demonstrated the profound effect of the cholesterol-depleting agent, MCD, on ROS cholesterol content, DRM protein fractionation, Tα membrane association, and caveolin-1/Tα interactions. Under conditions that dramatically depleted cholesterol from ROS membranes, MCD incubation altered the buoyant density of DRM-associated proteins. The observed decrease in buoyancy of DRM-associated proteins by cholesterol depletion is consistent with MCD-mediated raft disruption reported in other cell types (*36*−*38*, *62*). It is unlikely to result from gross perturbation of ROS membrane structure as our cholesterol depletion paradigm did not result in significant extraction of phospholipids by MCD, in agreement with a recently published report on cholesterol depletion of ROS (*39*). In addition to altering DRM protein fractionation, cholesterol depletion resulted in solubilization of a tightly associated pool of Tα from ROS membranes. The extraction of proteins by MCD treatment has also been reported in a mouse T-lymphocyte cell line (*42*). However, our results are in conflict with those of Seno et al. (*7*), who showed that Tα was not extracted from DRMs following a 1 h incubation with 10 mM MCD on ice. In our paradigm, ROS membranes were incubated with 15 mM MCD at 37 °C for 1 h. It is possible that elevated temperature and higher concentrations of MCD are required to effectively solubilize Tα. In addition

to extracting a pool of Tα from ROS membranes, incubation with MCD was also found to disrupt the complex between caveolin-1 and Tα. This is in agreement with recent reports demonstrating that cholesterol depletion inhibits co-immunoprecipitation of Ras (*63*) and the sodium−calcium exchanger (*64*) with caveolins. These results suggest that cholesterol is important for the association of Tα with DRMs, generally, and with caveolin-1, specifically.

Previous studies have indicated that the partitioning of Tα to DRMs in ROS is inhibited by GTPγS (*7*, *8*). These findings are consistent with our inability to recover Tα in caveolin-1 immunoprecipitates from ROS incubated with 10 μM GTPγS (see Figure 9). Furthermore, caveolin-1 has been shown to preferentially interact with the inactive, GDP-bound form of other Gα subunits and to inhibit nucleotide exchange (*45*). This may also suggest that Tα associated with caveolin-1 in our studies is in an inactive (GDP-bound) form. Interestingly, Nair et al. (*8*) have reported that Tα, in complex with RGS9-1, colocalizes to DRMs in response to light, and they further demonstrate that nucleotide exchange on Tα is dramatically reduced in DRM fractions. A recent report has also demonstrated that rhodopsin activation is reduced when the cholesterol content of ROS disks is increased to 31 mol % (*39*). On the basis of our data, DRMs from ROS contain nearly 35 mol % cholesterol; therefore, rhodopsin activation and rhodopsin/transducin coupling efficiency would likely be reduced in these membranes, suggesting that DRMs are not likely to support phototransduction. This also suggests that, although a small amount of opsin is present in DRMs, this DRM-associated opsin pool is unlikely to be responsible for the light-dependent partitioning of transducin to DRMs. One model that is consistent with our data and other published reports is that, following light activation and subsequent hydrolysis of GTP, Tα devoid of T$\beta\gamma$ [and possibly in a complex with RGS9-1 (*8*)] is localized to DRMs and is, therefore, capable of associating with caveolin-1 which is enriched in these membranes. Interaction of caveolin-1 thus may serve to sequester inactive Tα, preventing it from entering another cycle of light activation. Sequestering inactive Tα to DRMs by caveolin-1 may also have other functional downstream effects that are relevant to its differential localization (translocation) within photoreceptors in response to light exposure. Such a putative role has yet to be elucidated using an in vivo model.

ACKNOWLEDGMENT

We thank Dr. J. D. Ash for assistance with immunofluorescence imaging and for helpful discussions during the preparation of the manuscript. We also thank Dr. E. Floor at the University of Kansas for the generous gift of SV2 monoclonal antibody.

REFERENCES

1. Resh, M. D. (1999) Fatty acylation of proteins: new insights into membrane targeting of myristoylated and palmitoylated proteins, *Biochim. Biophys. Acta 1451*, 1−16.
2. Simons, K., and Ikonen, E. (1997) Functional rafts in cell membranes, *Nature 387*, 569−572.
3. Brown, D. A., and London, E. (1998) Functions of lipid rafts in biological membranes, *Annu. Rev. Cell Dev. Biol. 14*, 111−136.
4. Melkonian, K. A., Ostermeyer, A. G., Chen, J. Z., Roth, M. G., and Brown, D. A. (1999) Role of lipid modifications in targeting proteins to detergent-resistant membrane rafts. Many raft proteins are acylated, while few are prenylated, *J. Biol. Chem. 274*, 3910−3917.
5. Moffett, S., Brown, D. A., and Linder, M. E. (2000) Lipid-dependent targeting of G proteins into rafts, *J. Biol. Chem. 275*, 2191−2198.
6. Song, K. S., Sargiacomo, M., Galbiati, F., Parenti, M., and Lisanti, M. P. (1997) Targeting of a G alpha subunit (Gi1 alpha) and c-Src tyrosine kinase to caveolae membranes: clarifying the role of N-myristoylation, *Cell Mol. Biol. (Paris) 43*, 293−303.
7. Seno, K., Kishimoto, M., Abe, M., Higuchi, Y., Mieda, M., Owada, Y., Yoshiyama, W., Liu, H., and Hayashi, F. (2001) Light- and guanosine 5′-3-O-(thio)triphosphate-sensitive localization of a G protein and its effector on detergent-resistant membrane rafts in rod photoreceptor outer segments, *J. Biol. Chem. 276*, 20813−20816.
8. Nair, K. S., Balasubramanian, N., and Slepak, V. Z. (2002) Signal-dependent translocation of transducin, RGS9−1-Gbeta5L complex, and arrestin to detergent-resistant membrane rafts in photoreceptors, *Curr. Biol. 12*, 421−425.
9. Boesze-Battaglia, K., Dispoto, J., and Kahoe, M. A. (2002) Association of a Photoreceptor-specific Tetraspanin Protein, ROM-1, with Triton X-100-resistant Membrane Rafts from Rod Outer Segment Disk Membranes, *J. Biol. Chem. 277*, 41843−41849.
10. Yarfitz, S., and Hurley, J. B. (1994) Transduction mechanisms of vertebrate and invertebrate photoreceptors, *J. Biol. Chem. 269*, 14329−14332.
11. Arshavsky, V. Y., Lamb, T. D., and Pugh, E. N., Jr. (2002) G proteins and phototransduction, *Annu. Rev. Physiol 64*, 153−187.
12. He, W., Cowan, C. W., and Wensel, T. G. (1998) RGS9, a GTPase accelerator for phototransduction, *Neuron 20*, 95−102.
13. Philp, N. J., Chang, W., and Long, K. (1987) Light-stimulated protein movement in rod photoreceptor cells of the rat retina, *FEBS Lett. 225*, 127−132.
14. Whelan, J. P., and McGinnis, J. F. (1988) Light-dependent subcellular movement of photoreceptor proteins, *J. Neurosci. Res. 20*, 263−270.
15. Brann, M. R., and Cohen, L. V. (1987) Diurnal expression of transducin mRNA and translocation of transducin in rods of rat retina, *Science 235*, 585−587.
16. Sokolov, M., Lyubarsky, A. L., Strissel, K. J., Savchenko, A. B., Govardovskii, V. I., Pugh, E. N., Jr., and Arshavsky, V. Y. (2002) Massive light-driven translocation of transducin between the two major compartments of rod cells: a novel mechanism of light adaptation, *Neuron 34*, 95−106.
17. Baehr, W., Morita, E. A., Swanson, R. J., and Applebury, M. L. (1982) Characterization of bovine rod outer segment G-protein, *J. Biol. Chem. 257*, 6452−6460.
18. Kuhn, H. (1980) Light- and GTP-regulated interaction of GTPase and other proteins with bovine photoreceptor membranes, *Nature 283*, 587−589.
19. DeMar, J. C., Jr., Rundle, D. R., Wensel, T. G., and Anderson, R. E. (1999) Heterogeneous N-terminal acylation of retinal proteins, *Prog. Lipid Res. 38*, 49−90.
20. Kokame, K., Fukada, Y., Yoshizawa, T., Takao, T., and Shimonishi, Y. (1992) Lipid modification at the N terminus of photoreceptor G-protein alpha-subunit, *Nature 359*, 749−752.
21. Neubert, T. A., Johnson, R. S., Hurley, J. B., and Walsh, K. A. (1992) The rod transducin alpha subunit amino terminus is heterogeneously fatty acylated, *J. Biol. Chem. 267*, 18274−18277.
22. Neubert, T. A., and Hurley, J. B. (1998) Functional heterogeneity of transducin alpha subunits, *FEBS Lett. 422*, 343−345.
23. Bell, M. W., Desai, N., Guo, X. X., and Ghalayini, A. J. (2000) Tyrosine phosphorylation of the alpha subunit of transducin and its association with Src in photoreceptor rod outer segments, *J. Neurochem. 75*, 2006−2019.
24. Okamoto, T., Schlegel, A., Scherer, P. E., and Lisanti, M. P. (1998) Caveolins, a family of scaffolding proteins for organizing "pre-assembled signaling complexes" at the plasma membrane, *J. Biol. Chem. 273*, 5419−5422.
25. Schreiber, S., Fleischer, J., Breer, H., and Boekhoff, I. (2000) A possible role for caveolin as a signaling organizer in olfactory sensory membranes, *J. Biol. Chem. 275*, 24115−24123.
26. Kachi, S., Yamazaki, A., and Usukura, J. (2001) Localization of caveolin-1 in photoreceptor synaptic ribbons, *Invest. Ophthalmol. Visual Sci. 42*, 850−852.
27. Elliott, M. H., Desai, N., and Ghalayini, A. J. (2001) Caveolin, a photoreceptor rod outer segment protein that cofractionates with alpha subunit of transducin and c-Src, *Invest. Ophthalmol. Visual Sci. 42*, S184.

28. Godchaux, W., III, and Zimmerman, W. F. (1979) Soluble proteins of intact bovine rod cell outer segments, *Exp. Eye Res. 28*, 483−500.
29. Zimmerman, W. F., and Godchaux, W., III (1982) Preparation and characterization of sealed bovine rod cell outer segments, *Methods Enzymol. 81*, 52−57.
30. Bell, M. W., Alvarez, K., and Ghalayini, A. J. (1999) Association of the tyrosine phosphatase SHP-2 with transducin-alpha and a 97-kDa tyrosine-phosphorylated protein in photoreceptor rod outer segments, *J. Neurochem. 73*, 2331−2340.
31. Fliesler, S. J., Richards, M. J., Miller, C., and Peachey, N. S. (1999) Marked alteration of sterol metabolism and composition without compromising retinal development or function, *Invest. Ophthalmol. Visual Sci. 40*, 1792−1801.
32. Rouser, G., Fleischer, S., and Yamamoto, A. (1970) Two-dimensional thin layer chromatographic separation of polar lipids and determination of phospholipids by phosphorus analysis of spots, *Lipids 5*, 494−496.
33. Laemmli, U. K. (1970) Cleavage of structural proteins during the assembly of the head of bacteriophage T4, *Nature 227*, 680−685.
34. Muresan, V., Joshi, H. C., and Besharse, J. C. (1993) Gamma-tubulin in differentiated cell types: localization in the vicinity of basal bodies in retinal photoreceptors and ciliated epithelia, *J. Cell Sci. 104* (Part 4), 1229−1237.
35. Lisanti, M. P., Sargiacomo, M., and Scherer, P. E. (1999) Purification of caveolae-derived membrane microdomains containing lipid-anchored signaling molecules, such as GPI-anchored proteins, H.-Ras, Src-family tyrosine kinases, eNOS, and G-protein alpha-, beta-, and gamma-subunits, *Methods Mol. Biol. 116*, 51−60.
36. Fagan, K. A., Smith, K. E., and Cooper, D. M. (2000) Regulation of the Ca^{2+}-inhibitable adenylyl cyclase type VI by capacitative Ca^{2+} entry requires localization in cholesterol-rich domains, *J. Biol. Chem. 275*, 26530−26537.
37. Miura, Y., Hanada, K., and Jones, T. L. (2001) G(s) signaling is intact after disruption of lipid rafts, *Biochemistry 40*, 15418−15423.
38. Rybin, V. O., Xu, X., Lisanti, M. P., and Steinberg, S. F. (2000) Differential targeting of beta -adrenergic receptor subtypes and adenylyl cyclase to cardiomyocyte caveolae. A mechanism to functionally regulate the cAMP signaling pathway, *J. Biol. Chem. 275*, 41447−41457.
39. Niu, S. L., Mitchell, D. C., and Litman, B. J. (2002) Manipulation of cholesterol levels in rod disk membranes by methyl-beta-cyclodextrin: effects on receptor activation, *J. Biol. Chem. 277*, 20139−20145.
40. Gkantiragas, I., Brugger, B., Stuven, E., Kaloyanova, D., Li, X. Y., Lohr, K., Lottspeich, F., Wieland, F. T., and Helms, J. B. (2001) Sphingomyelin-enriched microdomains at the Golgi complex, *Mol. Biol. Cell 12*, 1819−1833.
41. Scheiffele, P., Roth, M. G., and Simons, K. (1997) Interaction of influenza virus haemagglutinin with sphingolipid-cholesterol membrane domains via its transmembrane domain, *EMBO J. 16*, 5501−5508.
42. Ilangumaran, S., and Hoessli, D. C. (1998) Effects of cholesterol depletion by cyclodextrin on the sphingolipid microdomains of the plasma membrane, *Biochem. J. 335* (Part 2), 433−440.
43. Glenney, J. R., Jr. (1992) The sequence of human caveolin reveals identity with VIP21, a component of transport vesicles, *FEBS Lett. 314*, 45−48.
44. Li, W. P., Liu, P., Pilcher, B. K., and Anderson, R. G. (2001) Cell-specific targeting of caveolin-1 to caveolae, secretory vesicles, cytoplasm or mitochondria, *J. Cell Sci. 114*, 1397−1408.
45. Li, S., Okamoto, T., Chun, M., Sargiacomo, M., Casanova, J. E., Hansen, S. H., Nishimoto, I., and Lisanti, M. P. (1995) Evidence for a regulated interaction between heterotrimeric G proteins and caveolin, *J. Biol. Chem. 270*, 15693−15701.
46. Murthy, K. S., and Makhlouf, G. M. (2000) Heterologous desensitization mediated by G protein-specific binding to caveolin, *J. Biol. Chem. 275*, 30211−30219.
47. Melkonian, K. A., Chu, T., Tortorella, L. B., and Brown, D. A. (1995) Characterization of proteins in detergent-resistant membrane complexes from Madin-Darby canine kidney epithelial cells, *Biochemistry 34*, 16161−16170.
48. Naslavsky, N., Stein, R., Yanai, A., Friedlander, G., and Taraboulos, A. (1997) Characterization of detergent-insoluble complexes containing the cellular prion protein and its scrapie isoform, *J. Biol. Chem. 272*, 6324−6331.
49. Sargiacomo, M., Sudol, M., Tang, Z., and Lisanti, M. P. (1993) Signal transducing molecules and glycosyl-phosphatidylinositol-linked proteins form a caveolin-rich insoluble complex in MDCK cells, *J. Cell Biol. 122*, 789−807.
50. Couet, J., Li, S., Okamoto, T., Ikezu, T., and Lisanti, M. P. (1997) Identification of peptide and protein ligands for the caveolin-scaffolding domain. Implications for the interaction of caveolin with caveolae-associated proteins, *J. Biol. Chem. 272*, 6525−6533.
51. Lambright, D. G., Sondek, J., Bohm, A., Skiba, N. P., Hamm, H. E., and Sigler, P. B. (1996) The 2.0 A crystal structure of a heterotrimeric G protein, *Nature 379*, 311−319.
52. Anderson, R. G. (1998) The caveolae membrane system, *Annu. Rev. Biochem. 67*, 199−225.
53. Smart, E. J., Graf, G. A., McNiven, M. A., Sessa, W. C., Engelman, J. A., Scherer, P. E., Okamoto, T., and Lisanti, M. P. (1999) Caveolins, liquid-ordered domains, and signal transduction, *Mol. Cell Biol. 19*, 7289−7304.
54. Carman, C. V., Lisanti, M. P., and Benovic, J. L. (1999) Regulation of G protein-coupled receptor kinases by caveolin, *J. Biol. Chem. 274*, 8858−8864.
55. Bridges, C. C., El Sherbeny, A., Roon, P., Ola, M. S., Kekuda, R., Ganapathy, V., Camero, R. S., Cameron, P. L., and Smith, S. B. (2001) A comparison of caveolae and caveolin-1 to folate receptor alpha in retina and retinal pigment epithelium, *Histochem. J. 33*, 149−158.
56. Guy, G. R. (1999) in *The Protein Protocols Handbook* (Walker, J. M., Ed.) pp 329−335, Humana Press, Totowa, NJ.
57. Oh, P., and Schnitzer, J. E. (2001) Segregation of heterotrimeric G proteins in cell surface microdomains. G(q) binds caveolin to concentrate in caveolae, whereas G(i) and G(s) target lipid rafts by default, *Mol. Biol. Cell 12*, 685−698.
58. Fliesler, S. J., and Anderson, R. E. (1983) Chemistry and metabolism of lipids in the vertebrate retina, *Prog. Lipid Res. 22*, 79−131.
59. Guzzi, F., Zanchetta, D., Chini, B., and Parenti, M. (2001) Thioacylation is required for targeting G-protein subunit G(o1alpha) to detergent-insoluble caveolin-containing membrane domains, *Biochem. J. 355*, 323−331.
60. Galbiati, F., Volonte, D., Meani, D., Milligan, G., Lublin, D. M., Lisanti, M. P., and Parenti, M. (1999) The dually acylated NH2-terminal domain of gi1alpha is sufficient to target a green fluorescent protein reporter to caveolin-enriched plasma membrane domains. Palmitoylation of caveolin-1 is required for the recognition of dually acylated g-protein alpha subunits in vivo, *J. Biol. Chem. 274*, 5843−5850.
61. Wedegaertner, P. B., Wilson, P. T., and Bourne, H. R. (1995) Lipid modifications of trimeric G proteins, *J. Biol. Chem. 270*, 503−506.
62. Becher, A., White, J. H., and McIlhinney, R. A. (2001) The gamma-aminobutyric acid receptor B, but not the metabotropic glutamate receptor type-1, associates with lipid rafts in the rat cerebellum, *J. Neurochem. 79*, 787−795.
63. Kranenburg, O., Verlaan, I., and Moolenaar, W. H. (2001) Regulating c-Ras function. cholesterol depletion affects caveolin association, GTP loading, and signaling, *Curr. Biol. 11*, 1880−1884.
64. Bossuyt, J., Taylor, B. E., James-Kracke, M., and Hale, C. C. (2002) Evidence for cardiac sodium−calcium exchanger association with caveolin-3, *FEBS Lett. 511*, 113−117.

BI027162N